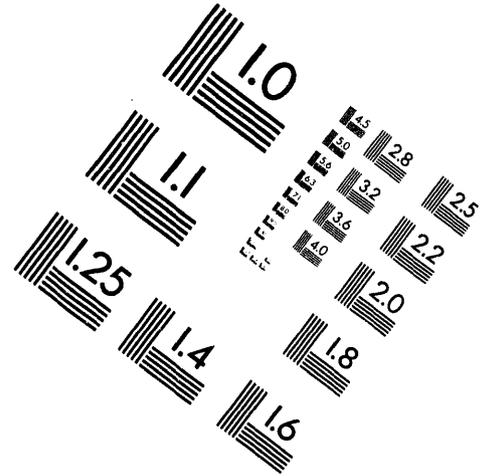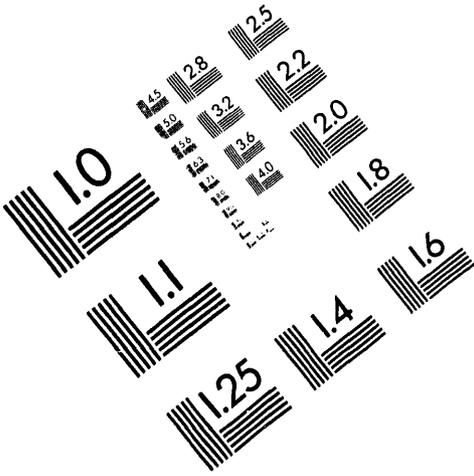# AIIM

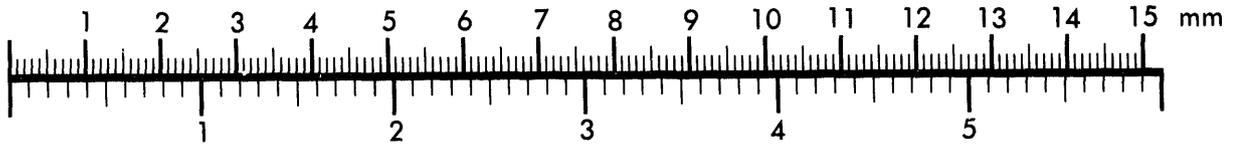**Association for Information and Image Management**
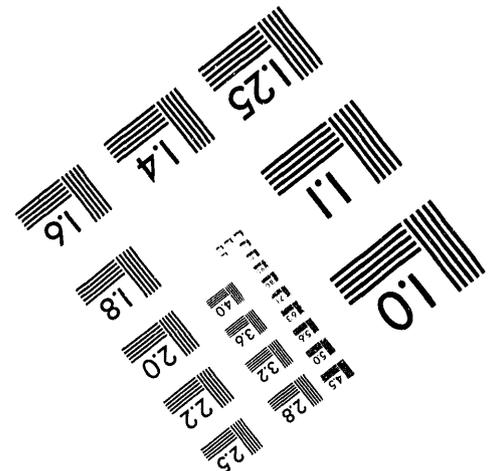
1100 Wayne Avenue, Suite 1100
Silver Spring, Maryland 20910

301/587-8202

Centimeter

Inches
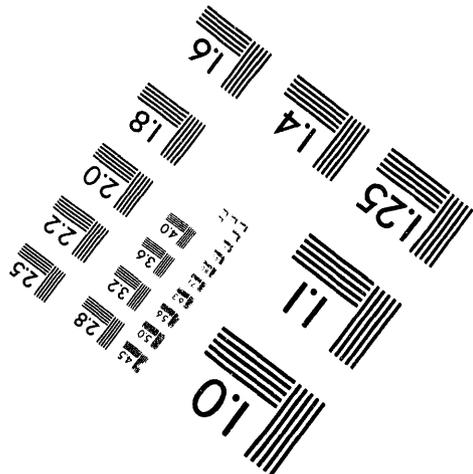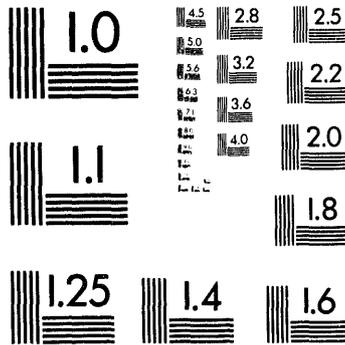
MANUFACTURED TO AIIM STANDARDS
BY APPLIED IMAGE, INC.

Conf-940748--48

LA-UR- 94-2561

Title: ACCOUNTING FOR SEGMENT CORRELATIONS IN SEGMENTED GAMMA-RAY SCANS

Author(s): G. A. Sheppard, T. H. Prettyman, and E. C. Piquette

Submitted to: Institute of Nuclear Materials Management
35the Annual Meeting
Naples, Florida
Jullt 17-20, 1994
(FULL PAPER)

Los Alamos
NATIONAL LABORATORY

MASTER

DISTRIBUTION OF THIS DOCUMENT IS UNLIMITED

ACCOUNTING FOR SEGMENT CORRELATIONS IN SEGMENTED GAMMA-RAY SCANS

G. A. Sheppard, T. H. Prettyman, and E. C. Piquette
Los Alamos National Laboratory
Los Alamo, NM 87545 USA

ABSTRACT

In a typical segmented gamma-ray scanner (SGS), the detector's field of view is collimated so that a complete horizontal slice or segment of the desired thickness is visible. Ordinarily, the collimator is not deep enough to exclude gamma rays emitted from sample volumes above and below the segment aligned with the collimator. This can lead to assay biases, particularly for certain radioactive-material distributions. Another consequence of the collimator's low aspect ratio is that segment assays at the top and bottom of the sample are biased low because the detector's field of view is not filled. This effect is ordinarily countered by placing the sample on a low-Z pedestal and scanning one or more segment thicknesses below and above the sample. This takes extra time, however. We have investigated a number of techniques that both account for correlated segments and correct for end effects in SGS assays. Also, we have developed an algorithm that facilitates estimates of assay precision. Six calculation methods have been compared by evaluating the results of thousands of simulated assays for three types of gamma-ray source distribution and ten masses. We will report on these computational studies and their experimental verification.

INTRODUCTION

With a conventional Segmented gamma-ray scanner (SGS) the assay procedure involves dividing the cylindrical sample into a number of axial segments and measuring the count rates at selected gamma-ray energies from the sample's contents as well as from an external source shining through the sample.[1-2] The segmentation is to partially account for vertical inhomogeneity in the sample. Radial inhomogeneities are partially mitigated by rotating the sample during data acquisition. It is assumed that the gamma-emitting nuclides and the matrix in which they reside are uniformly distributed in a segment, and that gamma-ray data from neighboring segments have no consequential influence on the assay. For segments that are not near the top or bottom of homogeneous samples and when

calibration standards are homogeneous, the latter assumption is valid. However, when neighboring segments differ significantly in matrix density or source distribution (or are absent, as is the case at the top and bottom of the sample), it is not safe to assume that a bias-free result can be obtained when the contributions of neighboring samples are not properly accounted for.

GENERATION OF DATA SET

To provide a suite of data upon which to test algorithms that account for segment correlations, we computer-generated the SGS counting data for 6000 mock assays. We assumed an SGS geometry similar to that of a commercial system collimated to allow a relatively large vertical field of view (the collimator is 2 in. high and only 4 in. deep). The model sample we used was a 24-in.-diameter container, 20 in. high, and divided into 10 segments. The attenuating matrix was assumed to be uniform throughout the container with a transmission of 0.1 at 185.7 keV. The nominal counts $I = 2500$ and $I_0=25000$, from which the transmission $T = I/I_0$ was computed, were assumed to vary according to Poisson statistics. Passive counts were assumed to be governed by Poisson statistics as well. Gross and continuum counts were simulated using a Poisson random number generator.

We studied three types of source distributions: all nuclear material distributed uniformly in the bottom segment only; a homogeneous distribution of the nuclear material through the entire sample volume; and a random segmented distribution, in which a known total mass of ^{235}U was distributed randomly among the sample segments. In all cases, the source distribution was uniform within a given segment. Each randomly distributed mock sample was unique.

Ten mass values, ranging from 0.09 g to 49 g of ^{235}U were assayed for distribution type. Each mock sample was assayed repeatedly (200 times) to determine the effect of counting statistics on the assay result. We used a range of masses so that we could observe the dependence on counting statistics of the mean assay result and its distribution. The acquisition time for each segment was 200 s, and the total counts for all ten segments ranged from approximately 125 for 0.09 g to 64 000 counts for 49 g of ^{235}U. The total mass and count rate of each successive sample doubled that of the previous sample.

METHOD DESCRIPTIONS

The computer-generated data for each of the 6000 assays (200 measurements at each of the ten ^{235}U masses, distributed each of three ways) were analyzed using each of six algorithms. We used a point-source calibration method,[4] instead of taking the conventional approach with homogeneous, distributed calibration standards.

No End Eff. This is the present method employed by most SGS systems. No end effect correction is employed and no segment correlations are assumed. For each segment, a correction factor for attenuation by the matrix is calculated as a function of the measured transmission through the diameter of the sample, assuming a simplified geometrical model of the detector, collimator, and sample.[3] This correction factor is applied to the full-energy interaction rate at the assay energy to yield a corrected rate for the segment. Corrected rates for all segments in a sample are summed and a calibration constant is applied to the result to arrive at the total mass of the gamma-emitting isotope in the sample container.

End Eff Corr. This technique involves the same type of isolated-segment attenuation correction as above, except that an additional algorithm is applied to correct for end effects. The program also performs an associated correction due to varying transmissions in adjacent segments (which is small with the assumed uniform matrix). This correction accounts for both the axial response of the SGS and path-length variations.

In the remaining techniques, the segments are not assumed to be independent. Each technique applies an algorithm that attempts to solve the system of equations that describes the convolved response arising from the segment aligned with the collimator and it refers to collimator the neighboring segments. These correlated-segment models assume that the mass contained in an individual segment is homogeneously distributed throughout the segment volume and that attenuation is constant within the segment and equal to that measured along a diameter through its center.

Singular Value Decomposition (SVD). This is a correlated-segment calculation that solves the 10 by 10 matrix system with an unconstrained linear least-squares technique using the singular value decomposition approach. The solution is unconstrained; negative mass values in individual segments are allowed.

Smooth. In this method, the passive counts for the ten segments are smoothed using an iterative two-point smoothing algorithm; then the SVD approach is applied.

Algebraic Reconstruction Technique (ART) . This is an algebraic reconstruction technique developed for computed tomography.[5] It is a constrained

iterative method of solving the system of equations for the correlated segment problem during which individual segment masses are constrained to be greater than zero. This study was performed using 500 iterations.

Maximum Likelihood-Expectation Maximization (ML-EM). This is another iterative method of calculating the correlated-segment problem. It assumes Poisson statistics in both net peak and background counts.[6] Again, 500 iterations were used.

RESULTS

We show three types of graphs. Figures 1 and 2 illustrate the relative difference between the mean results of the six methods mean results and the actual total masses. Figure 1 is for homogeneous distributions and Fig. 2 summarizes the assay results for samples in which all the ^{235}U is in the bottom segment. Results for random mass distributions are not summarized because they were virtually identical to those arising from homogeneous samples. This is to be expected, because the mean result from assays of a large number of samples in which the source mass is randomly distributed should approach the homogeneous case.

Figures 3 and 4 show the standard deviation of the assay results for each method, expressed as a percentage of the standard total mass. They indicate the precision of the methods and their relative susceptibility to counting statistics.

Figure 5 indicates the relative ability of the assay methods to recover the true distribution of mass within
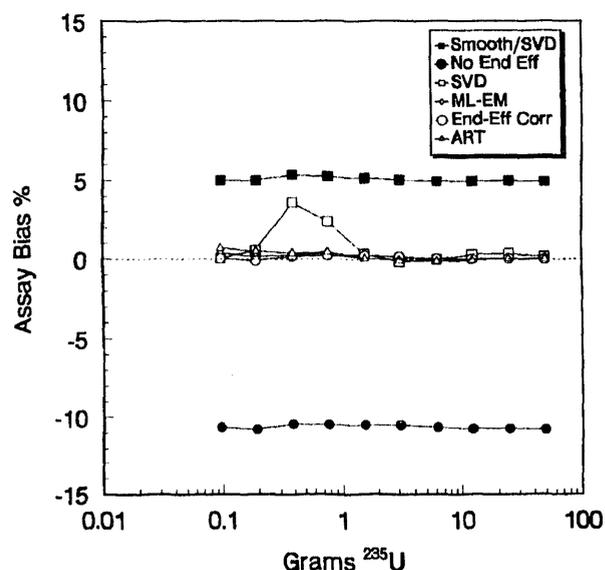

Fig. 1. For each of six analysis methods, relative assay bias as a function of mass of ^{235}U distributed homogeneously throughout the sample.
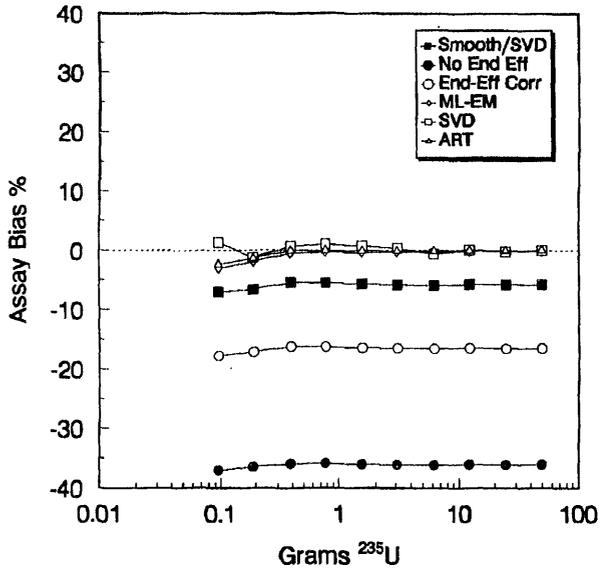
Fig. 2. For each of six analysis methods, relative assay bias as a function of mass of ^{235}U located in only the bottom segment of the sample.
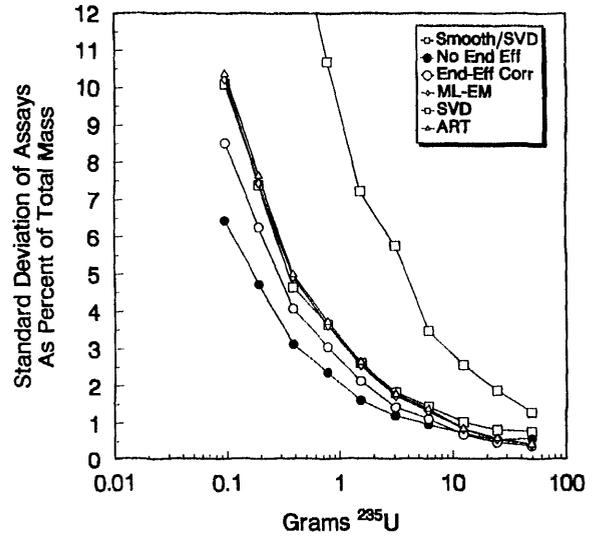
Fig. 4. For each of six analysis methods, standard deviation of the results of 200 assays at each of 10 masses of ^{235}U located in only the bottom segment of the sample.

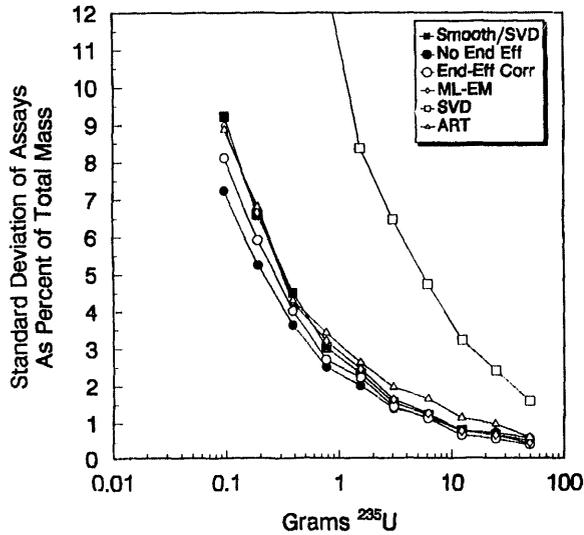Fig. 3. For each of six analysis methods, standard deviation of the results of 200 assays at each of 10 masses of ^{235}U distributed homogeneously throughout the sample.
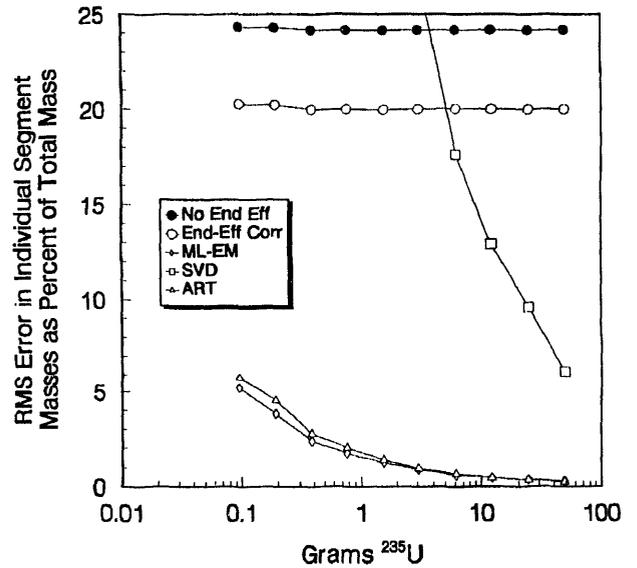

Fig. 5. For each of five analysis methods, root-mean-square error in individual segment masses, normalized to total mass, at each of 10 masses of ^{235}U located in only the bottom segment of the sample. Results of the smoothed SVD approach are off-scale.

the sample. It shows the relative root-mean- square deviations of the assayed segment mass from the true mass for all segments for the 200 assays at each total mass.

INTERPRETATION AND EVALUATION

Figures 1 and 2 show a wide variation of the absolute bias associated with the six methods. The conventional assay technique is biased low, the smoothed SVD approach is biased high, and the rest are bias-free. All the curves are comparatively flat except for the SVD results, which are attributable to the technique's sensitivity to statistical variations. Upon calibration, however, this absolute bias can be incorporated into the calibration constant of the system, after which only the relative bias (bias of a method relative to itself for different samples or count rates) is important.* The flatness of most of the curves in Figs. 1 and 2 is an indication of the very small relative bias arising from statistics. A reliable method would have the same bias on each graph, indicating that it is independent of distribution type. However, a comparison of Figs. 1 and 2 reveals that the conventional SGS assay method would yield a measurement result 28% low when analyzing a sample with all the source mass in the bottom segment, if calibrated using a homogeneous standard. The end-effect corrected version of the same technique would result in a -16% bias.

As Figs. 1 and 2 show, the ART and ML-EM methods produce results of equivalent quality for total mass. Figure 5 reveals the fact that the methods that do not account for segment correlations do not meet the challenge of accurately assaying a sample in which all of the source mass lies at the bottom. Only the ART and ML-EM methods appear to provide accurate assays of an arbitrary distribution, with ML-EM marginally outperforming ART.

It is remarkable that the unconstrained SVD technique produces the correct total mass despite significant variations in the solution (Figs. 1 and 2). The effect of the unconstrained solutions is evident in Figs. 3 and 4, where it is clear that the SVD approach yields a much poorer precision than the other methods studied. Also noteworthy in Figs. 3 and 4 is the fact that the precision of the conventional approach, whether corrected for end-effects or not, is not significantly better than average when normalized to its mean assay results, as opposed to the total reference mass.

EXPERIMENTAL VERIFICATION

To test the validity of our calculated results, we loaded 208-L and 113-L drums with our "pillow" stan-

---

* Absolute bias becomes important if one desires the system to be calibrated with a point source standard.

dards. These standards, each containing 4.64 g of ^{235}U, were created in 1972 by sprinkling measured amounts of HEU in oxide form on low-density paper as it was stuffed into plastic bags lining 1-gal. paint cans. To achieve a "uniform" distribution of the pillow standards in a drum, we stacked them with polystyrene-foam spacer blocks to achieve an even distribution of the standards through the drum volume. We also experimented with nonuniform distributions by bunching the pillows in the bottom or the middle of the drum, using foam spacer blocks as required. Data were taken using a commercial SGS calibrated with uniform, distributed standards. We analyzed the results using the ML-EM method and the conventional method, with and without end-effect corrections. Results are depicted in Fig. 6. The average results, normalized to the reference value, were 1.0018 ± 0.0278 for the ML-EM method, 0.9909 ± 0.0285 for the conventional method with end-effect corrections, and 0.9776 ± 0.0620 for the conventional method without end-effect corrections. Note that, in every case, drums loaded with a single layer of pillow standards in the bottom assayed low by the conventional method without end-effect corrections.
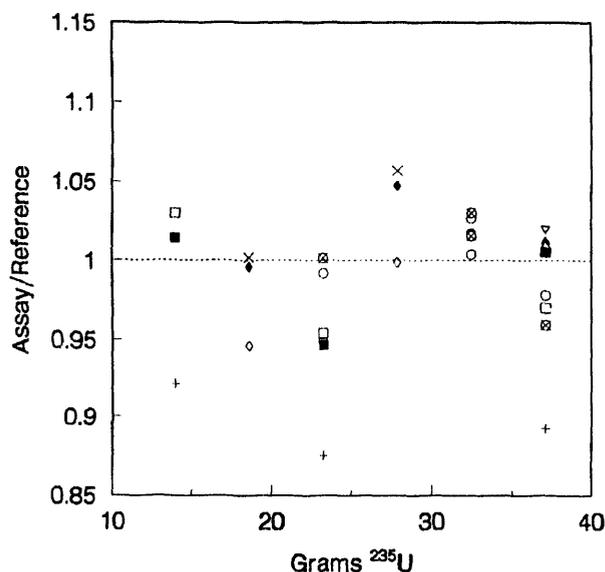

Fig. 6. For different configurations of ^{235}U pillow standards in 113-L and 208-L drums, relative assay bias as a function of ^{235}U in the drum. Solid symbols indicate assay results using the ML-EM approach. Open symbols correspond to results obtained by performing a conventional analysis and applying end-effect corrections. For drums in which there is a single layer of pillows in the bottom and + represent the results obtained using the ML-EM approach, the conventional approach with end-effect correction, and the uncorrected conventional approach, respectively.

REFERENCES

1. E. R. Martin, D. F. Jones, and J. L. Parker, "Gamma-Ray Measurements with the Segmented Gamma Scan," Los Alamos Scientific Laboratory report LA-7059-M (December 1977).

2. "Standard Test Method for Nondestructive Assay of Special Nuclear Material in Low Density Scrap and Waste by Segmented Passive Gamma-Ray Scanning," *Annual Book of ASTM Standards*, Vol. 12.01, C 1133-89 (1992).

3. J. L. Parker, "The Use of Calibration Standards and the Correction for Sample Self-Attenuation in Gamma-Ray Nondestructive Assay," Los Alamos National Laboratory report LA-10045, Rev (November 1986).

4. G. A. Sheppard and E. C. Piquette, "Point-Source Calibration of a Segmented Gamma-Ray Scanner," to be presented at the Institute of Nuclear Materials Management (INMM), Annual Meeting, Naples, Florida, July 17-20, 1994, Los Alamos National Laboratory document LA-UR-94-2482.

5. A. C. Kak and M. Slaney, *Principles of Computerized Tomographic Imaging* (IEEE Press, New York, 1987), pp. 283-284.

6. T. H. Prettyman, R. A. Cole, R. J. Estep, and G. A. Sheppard, "A Maximum-Likelihood Reconstruction Algorithm for Tomographic Gamma-Ray Nondestructive Assay," presented at the 1994 Symposium on Radiation Measurements and Applications, Ann Arbor, MI, May 16-19, 1994, Los Alamos National Laboratory document LA-UR-94-1650.

END

DATE FILMED
9 /28 /94